Polymer 49 (2008) 3884–3891

Contents lists available at ScienceDirect

Polymer

journal homepage: www.elsevier.com/locate/polymer

Coagent-induced transformations of polypropylene microstructure: Evolution of bimodal architectures and cross-linked nano-particles

J. Scott Parent [a,*], Saurav S. Sengupta [a], Michael Kaufman [a], Bharat I. Chaudhary [b]

[a] Department of Chemical Engineering, Queen's University, Kingston, Ontario, Canada K7L 3N6
[b] The Dow Chemical Company, 1 Riverview Drive, Somerset, NJ 08873, USA

ARTICLE INFO

Article history:
Received 30 April 2008
Received in revised form 23 June 2008
Accepted 2 July 2008
Available online 15 July 2008

Keywords:
Polypropylene
Long-chain branching
Precipitation polymerization

ABSTRACT

Polypropylene is transformed by simultaneous, radical-mediated chain scission and cross-linking to generate branched architectures. While macroradical fragmentation reduces the molar mass of the dominant chain population, cross-linking by triallyl trimesate (TAM) activation yields a minority population of hyper-branched chains that is less susceptible to molecular weight loss. This disparity in chain reactivity leads to bimodal molecular weight and branching distributions. Furthermore, a precipitation polymerization of TAM can proceed concurrently with PP branching to produce a low yield of cross-linked, TAM-rich nano-particles. The mechanisms through which unimodal composition and molecular weight distributions evolve toward a bimodal condition are discussed, along with the factors that lead to particle formation.

1. Introduction

Branched architectures are desirable whenever melt strength and elongational viscosity are key material properties [1]. The deficiency of linear polypropylene (PP) in these respects [2] has fuelled interest in the preparation and characterization of PP derivatives that possess varying degrees of long-chain branching [3,4]. A simple synthetic route involves solvent-free reactive processing wherein polyfunctional coagents such as triallyl trimesate (TAM, Scheme 1) are activated by alkyl peroxides at elevated temperature [5]. Using this methodology, linear PP materials are transformed by radical-mediated chain scission and coagent-induced cross-linking, the balance of which dictates the resulting distributions of molecular weight, branch length, and branch frequency.

In addition to supporting curing technology for the synthesis of thermoset PP products [6], coagent-mediated cross-linking has been used to prepare functional PP materials. For example, maleic anhydride has been co-grafted with triallyl isocyanurate to PP [7], and we have recently detailed a range of techniques that use triallyl trimellitate and its derivatives to introduce moisture-curing alkoxysilane functionality [8]. This approach to PP modification seeks to minimize changes in melt viscosity by introducing only as much cross-linking as is required to offset the effects of fragmentation.

Notwithstanding the widespread interest in PP branching, curing, and functionalization, there exists very little fundamental information regarding this important branch of polymer chemistry. The present work is concerned with the radical chemistry of allylic ester coagents acting upon PP. Detailed ^{1}H NMR analysis of atactic-PP products is used to identify the predominant mode of TAM activation, and to quantify the extent of cross-linking and radical-induced chain scission. Size exclusion chromatography coupled with light scattering analysis is used to reveal molecular weight and composition distributions of coagent-modified products, while optical and scanning electron microscopy are used to characterize an unexpected precipitation polymerization process that can operate concurrently with PP graft modification.

2. Experimental

2.1. Materials

Triallyl trimesate (TAM, 99%, Monomer Polymer Inc) and dicumyl peroxide (DCP, 98%, Sigma–Aldrich) were used as-received. Atactic polypropylene (a-PP, $M_n = 4700$ g/mol, polydispersity = 2.0, Scientific Polymer products) was hydrogenated prior to use by treatment of a hexane solution with platinum supported on carbon at 20 bar H_2, 100 °C for 50 h, after which the polymer was recovered by precipitation from acetone and dried under vacuum. An additive-free isotactic polypropylene homopolymer (i-PP, $M_n =$ 70,700 g/mol, polydispersity = 5.5) was used as supplied by the Dow Chemical Company.

* Corresponding author. Tel.: +1 613 533 6266; fax: +1 613 533 6637.
E-mail address: parent@chee.queensu.ca (J.S. Parent).

0032-3861/$ – see front matter © 2008 Elsevier Ltd. All rights reserved.
doi:10.1016/j.polymer.2008.07.007

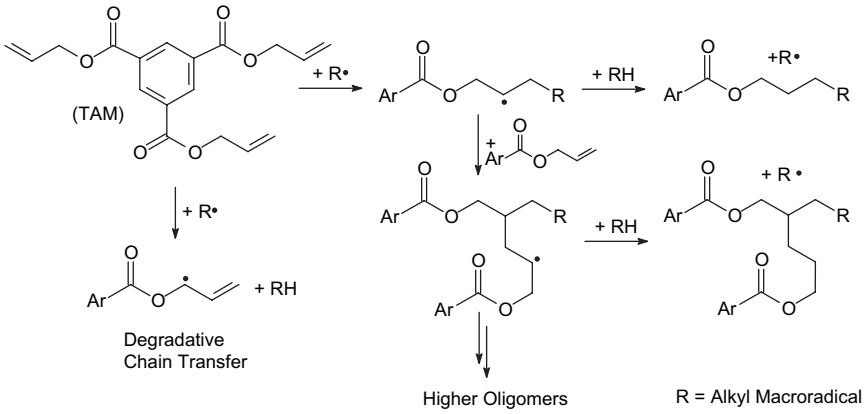

Scheme 1. Modes of TAM Activation.

2.2. Instrumentation and analysis

NMR spectra were recorded with a Bruker AM-600 spectrometer (600.17 MHz ^{1}H, 150.92 MHz ^{13}C) in d_8-toluene at 50 °C for a-PP products, with chemical shifts referenced to tetramethylsilane. FT-IR analysis was conducted with a Nicolet Avatar 360 FT-IR ESP spectrometer. Scanning electron microscopy analysis of gold-sputtered samples was performed using a JEOL JSM-840 instrument. Elemental analysis for carbon, hydrogen and oxygen contents was conducted by Canadian Microanalytical Service Ltd of Delta, British Columbia, Canada.

Low-temperature GPC analysis of filtered samples of a-PP and its derivatives was conducted in THF at 40 °C and 1 ml/min using a Waters 2960 separation module equipped with a Styragel guard column and four Styragel columns HR(0.5), HR(1.0), HR(3.0), HR(4.0) in series. A Waters 410 differential refractometer and a Wyatt Technology DAWN EOS laser photometer. Absolute molecular weights were calculated using knowledge of a d*n*/d*c* value of 0.0888 ml/g for a-PP in THF at 690 nm, which was determined independently using a DAWN Optilab rEX instrument from Wyatt.

High-temperature triple detection GPC analysis of i-PP and its derivatives was conducted in 1,2,4-trichlorobenzene (TCB) at 160 °C and 1 ml/min using a Polymer Labs PL 220 instrument equipped with a Precision Detectors (Model 2040) light scattering instrument, for which the 15° angle detector was used for calculation purposes. The viscometer was a Viscotek model 210R detector. The column bank consisted of four 7.8 × 300 mm PL gel 20 μ Mixed A beds. The d*n*/d*c* value used for calculating molecular weights from the light scattering data was 0.104 ml/g. The detector responses were calibrated using an internally validated polyethylene standard. The samples were dissolved in BHT stabilized TCB at 160 °C for approximately 2.5 h prior to analysis.

2.3. Atactic-PP-g-triallyl trimesate

a-PP (2 g) and the desired amount of TAM were degassed in a round bottom flask by three cycles of vacuum evacuation and N_2 atmosphere replacement. The mixture was immersed in an oil bath at 170 °C and stirred to give a homogeneous mixture. This homogeneous condition was confirmed by optical microscopy of an a-PP mixture containing 3 wt% TAM. The required amount of DCP was introduced and left to decompose for 15 min, yielding a-PP-*g*-TAM. The product (1 g) was purified from residual TAM and initiator byproducts by dissolving in xylene (4 ml), precipitating from acetone (25 ml), and drying under vacuum. The composition of these unfractionated products was determined by ^{1}H NMR spectroscopy. Downfield ^{1}H NMR (d_8-toluene, 50 °C): δ 4.30–4.50 (t, 2H, –OCH_2–), δ 4.65–4.90 (d, 2H, vinylidene=CH_2), δ 4.8–4.85 (d, 2H, –CH_2CH=CH_2), δ 6.05–6.20 (m, 2H, –C*H*=CH_2), δ 8.70–8.90 (s, 3H, aromatic=CH–).

Fractionation of a-PP-*g*-TAM samples (2 g) into THF-extracted and hyper-branched components was accomplished by stirring with THF (20 ml) at 25 °C for 3 h to give a cloudy solution. The mixture separated into a clear solution and a solid residue upon standing for 24 h. The extraction solution was decanted from the solids and precipitated from acetone (80 ml) to yield THF-extracted material, which was then dried under vacuum. The residue was washed twice with THF (5 ml) and dried under vacuum to give the hyper-branched fraction. Amounts of alkyl ester, vinylidene fragmentation product, grafted aromatic, and residual allyl groups were determined by quantitative integration of ^{1}H NMR (d_8-toluene, 50 °C) spectra, as detailed above. Cross-linked nano-particles were isolated from the hyper-branched fraction by repeated washing with hot toluene to constant mass. The residual particles were dried under vacuum, sonicated in an acetone suspension and dispersed on a glass slide.

Optical microscopy experiments were conducted within a Linkam CSS 450 hot-stage apparatus attached to an Olympus BX51 microscope that was equipped with a Sony DXC-390 CCD camera. a-PP (2 g), TAM (0.06 g) and DCP (0.01 g) were stirred in an oil bath at 100 °C to give a homogeneous mixture, which was transferred to a hot-stage that was preheated to 100 °C. The sample gap was closed to 3 mm prior to raising the temperature rapidly to 170 °C. Images were recorded at 30 s intervals for 20 min.

2.4. Isotactic-PP-g-TAM

Ground i-PP (40 g) was coated with an acetone solution containing the desired amount of TAM and DCP. Acetone was evaporated, and the polymer mixture was charged to a Haake Polylab R600 internal batch mixer at 180 °C for 7 min at 60 rpm to give i-PP-*g*-TAM. The product (1 g) was purified by dissolving in xylene (5 ml) at 130 °C, precipitating from acetone (25 ml) and drying under vacuum. Grafted TAM contents were determined by FT-IR absorbance integrations of the 670–1751 cm^{-1} absorbance derived from the coagent relative to a 422–496 cm^{-1} internal standard region originating from the resin.

Fractionation of i-PP-*g*-TAM samples was accomplished by extracting 0.5 g of material using 120 mesh sieve cloth in refluxing xylenes (40 ml) for 6 h. The xylene-soluble fraction was recovered by precipitating from acetone (200 ml) and dried under vacuum. The residue was dried under vacuum to constant weight, with the yield of insoluble gel reported as the weight percent of the crude sample mass. TAM-rich particles were isolated by dissolving

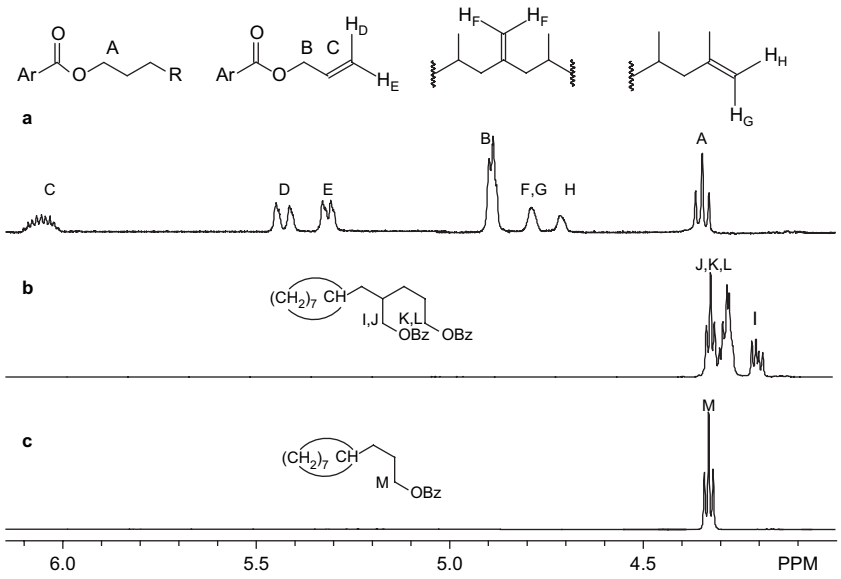

Fig. 1. Downfield ^{1}H NMR spectra (d_8-toluene, 50 °C) of (a) unfractionated a-PP-*g*-TAM (Experiment C, Table 1); (b) allyl benzoate dimer and (c) allyl benzoate–cyclooctane mono-adduct [8].

i-PP-*g*-TAM in hot xylenes and allowing particulate matter to adsorb on the glass surface of the vessel before decanting off the solution and accompanying gel.

3. Results

Unlike acrylate and styrenic systems, allylic esters are not prone to excessive homopolymerization [9] due to the limited reactivity of an unactivated olefin with respect to radical addition [10,11], and the inhibitory effects imposed by degradative allylic hydrogen atom abstraction (Scheme 1) [12,13]. Homopolymerization is further suppressed when allylic esters are activated in a large excess of hydrocarbon, such that hydrogen atom transfer can compete with allyl groups for monomer-derived radical adducts [8]. Our studies begin with spectroscopic analyses of low molecular weight, atactic-PP (a-PP) products to determine the main pathways of TAM consumption.

3.1. Atactic-PP derivatives

The products of a-PP addition to TAM are soluble in d_8-toluene at 50 °C, and can therefore be subjected to analysis by solution NMR spectroscopy. Fig. 1 illustrates a ^{1}H NMR spectrum of an unfractionated sample of purified a-PP-*g*-TAM, along with spectra derived from a simple allyl benzoate–cyclooctane adduct, and a corresponding allyl benzoate dimer. The methylene group adjacent to oxygen is of particular analytical value, as it provides insight into the nature of a coagent graft. Whereas a single addition product produces a simple triplet, the heteroatom region of an oligomer spectrum is complicated by the presence of multiple alkyl ester groups and their accompanying asymmetric centers. The observed triplet at δ 4.32 ppm in the a-PP-*g*-TAM spectrum is evidence of simple PP + TAM adducts that result from macro-radical addition to coagent, and hydrogen atom donation to the resulting alkyl radical (Scheme 1). Other modes of coagent activation, such as oligomerization and degradative chain transfer, may affect reaction yields, but do not contribute greatly to product distributions.

^{1}H NMR analysis of unfractionated a-PP-*g*-TAM samples also provided estimates of the overall conversion of TAM to PP grafts, and the concentration of alkyl ester functionality (grafted allyl ester groups) and vinylidene end-groups (RMeC=CH_2) within reaction products (Table 1). The latter served as an indicator of the extent of radical-mediated chain scission. We note, however, that vinylidene functionality may be reactive with respect to radical addition and/or allylic hydrogen abstraction, yielding products that cannot be quantified. Our values reflect the minimum extent of PP fragmentation.

Table 1
Properties of a-PP-*g*-TAM products[a,b]

	[DCP][c] (wt%)	[TAM][c] (wt%)	Unfractionated product			THF-extracted fraction						Hyper-branched fraction			
			TAM Conv (%)	Alkyl ester (μmol/g)	R_2C=CH_2 (μmol/g)	Wt%	M_n (g/mol)	M_n/M_w	Bound TAM (wt%)	Alkyl ester (μmol/g)	R_2C=CH_2 (μmol/g)	Wt (%)	Bound TAM (wt%)	Alkyl ester (μmol/g)	R_2C=CH_2 (μmol/g)
A	–	–	–	–	0	–	4700	2.0	–	–	–	–	–	–	–
B	0.3	0.0	–	–	30	–	3200	2.6	–	–	–	–	–	–	–
C	0.1	3.0	20	24	12	>99	3400	2.6	0.6	23	13	<1	–	–	–
D	0.3	3.0	31	54	20	94	4400	2.3	0.3	12	3	6[d]	11	682	326
E	0.5	3.0	38	72	31	95	4400	2.4	0.8	32	4	5[d]	7	642	422
F	0.3	1.0	69	47	26	>99	4200	2.2	0.7	47	25	<1	–	–	–
G	0.3	5.0	32	86	13	88	6100	2.1	0.2	5	1	12[e]	13	699	104

[a] T = 170 °C, 15 min.
[b] ^{1}H NMR analysis conducted in d_8-toluene at 50 °C.
[c] DCP (0.3 wt%) = 11.1 μmol/g, 3.0 wt% TAM = 91 μmol/g.
[d] Includes trace nano-particle yield.
[e] Includes 1 wt% nano-particle yield.

Spectroscopic analysis of unfractionated a-PP-*g*-TAM samples confirmed the expected relationships between alkyl ester yields and reagent loadings. For example, the use of relatively high peroxide loadings (Experiment E, Table 1) or relatively high coagent concentrations (Experiment G) increased the yield of alkyl ester. Similarly, elevated initiator loadings increased the yield of vinylidene fragmentation products (12 μmol/g versus 31 μmol/g for Experiments C and E, respectively), thereby affecting a different balance between chain scission and cross-linking.

One observation of note is the apparent suppression of chain fragmentation by the presence of TAM. The vinylidene end-group concentration fell from 30 μmol/g when 0.3 wt% DCP was activated in the absence of TAM, to 26 μmol/g, 20 μmol/g and 13 μmol/g when TAM was used in 1.0 wt%, 3.0 wt% and 5.0 wt% amounts, respectively. A plausible explanation involves a decline in the tertiary PP macroradical population due to the trapping of these intermediates by coagent. By diverting a portion of macroradicals, the frequency of chain scission may be reduced. Similar arguments have been put forth by Ciardelli and coworkers, who employed furan derivatives as macroradical traps to promote PP cross-linking [14] and by Cartier and Hu in their attempts to influence PP maleation selectivity using styrene as a co-monomer [15].

Whole a-PP-*g*-TAM samples were soluble in warm toluene, but room temperature THF had difficulty dissolving high molecular weight polymer chains. This provided a means of separating a-PP-*g*-TAM by molecular weight/composition into "THF-extracted" and "hyper-branched" fractions. The results compiled in Table 1 divide our samples in two groups – products that were readily dissolved in THF at room temperature (C and F), and those that contained isolable amounts of unextracted products (D, E, and G).

Our examination of these fractions begins with the GPC profiles of unmodified a-PP and the THF-extracted a-PP-*g*-TAM material derived from Experiment G, Table 1. The refractive index detector responses illustrated in Fig. 2 reveal only subtle differences between these filtered samples. The small refractive index signal recorded for a-PP-*g*-TAM in the 21–23 ml elution volume range is evidence of a new, high molecular weight population, and there appears to be a slight increase in this derivative's low molecular weight tail. Nevertheless, graft modification did not affect molecular weights to the degree reported in most studies of peroxide-initiated PP modification [16]. The insensitivity of our system stems from the low molecular weight of our starting material. A polymer with a M_n of 4700 g/mol provides 213 μmol of PP chains per gram, which exceeds the vinylidene (12–31 μmol/g) and alkyl ester (24–86 μmol/g) levels in our products. Therefore, the kinetic chain length of chain scission and cross-linking was insufficient to affect the whole a-PP chain population, given the amount of initiator employed.

Light scattering analysis revealed much about the structure of a-PP-*g*-TAM derivatives. Although the refractive index detector indicated that very little polymer eluted in the 20–23 ml range, this material generated an intense light scattering detector response (Fig. 2). The molar mass of this chain population exceeded 200 kg/mol, which represents about two orders of magnitude growth from the starting material. Given that this material was built from 5 kg/mol chains, it must possess a branch-on-branch architecture that is best classified as "hyper-branched". Note that hyper-branched material is sparingly soluble in room temperature THF, and its amount is not reflected by GPC measurements. The data reported in Table 1 were derived from gravimetric analyses of THF extractions.

Fig. 3 presents light scattering detector responses for the THF-soluble components of all a-PP-*g*-TAM products. The plots reveal the inherent bimodality produced by coagent-assisted PP modifications, as all samples showed some evidence of a new, high-mass chain population. Not surprisingly, a-PP-*g*-TAM samples that

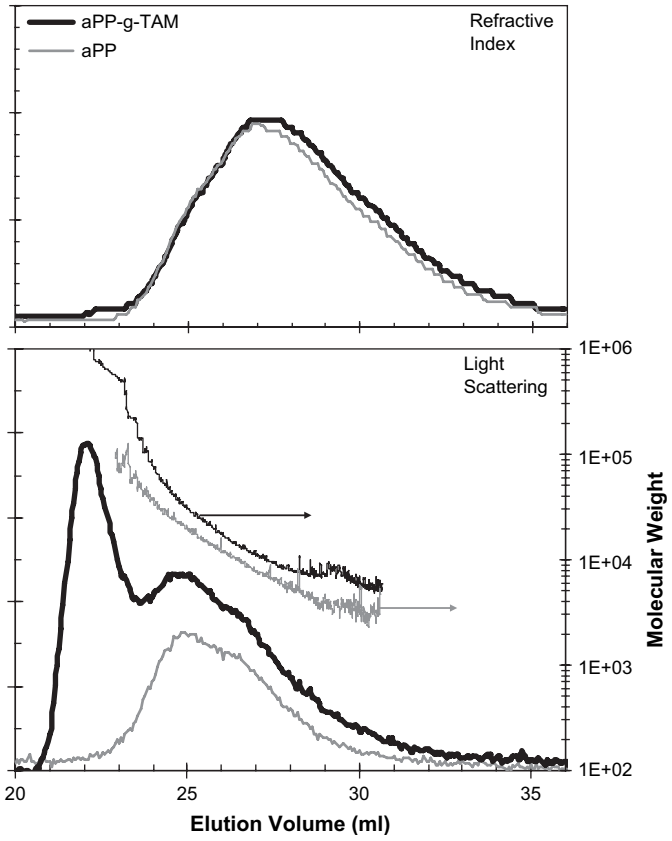

Fig. 2. Low-temperature GPC profiles for filtered samples of a-PP and the THF-extracted component of its TAM derivative (Table 1, Experiment G).

contained isolable amounts of hyper-branched material (D, E, and G) produced the most intense light scattering response at low elution volumes. They also contained the highest concentration of grafted allylic ester (Table 1). However, these cross-links were concentrated within the hyper-branched fraction, while the extracted fraction contained relatively small amounts of bound coagent and fragmentation product. This suggests that hyper-branched material is produced at the expense of the functionalized chains present within the extractable population.

The high concentration of alkyl ester within hyper-branched chains is consistent with the molecular weight of this material, but it is interesting to note that the distribution of vinylidene functionality is similarly concentrated in the hyper-branched fraction (Table 1). It is apparent that radical activity – both cross-linking and fragmentation – is more intense amongst the hyper-branched population. Selectivity for the fragmentation of high-mass chains is well documented in the PP degradation literature [16], and this point will be reexamined in the context of branching chemistry within Section 4.

We noted that samples that contained an isolable amount of hyper-branched material had a creamy appearance. A mixture of a-PP and 3.0 wt% of TAM is homogeneous at 170 °C when viewed with an optical microscope. However, when it is activated with 0.5 wt% DCP (Experiment E, Table 1) it loses optical transparency in concert with the reaction extent, as dictated by the half-life of the peroxide (Fig. 4). These images did not change colour or lose clarity, however, suggesting that the observed turbidity resulted from a dispersed phase with very small dimensions. The THF extract of this product was analyzed by NMR and optical microscopy, which confirmed that the matrix is as transparent as the starting material. Turbidity arises from the creation of a new phase.

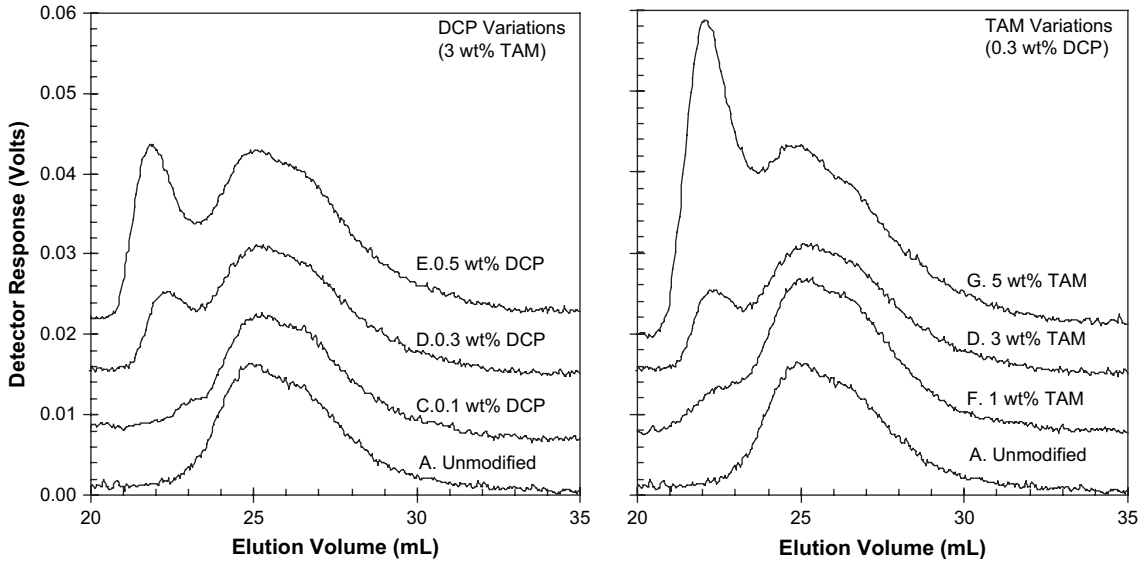

Fig. 3. Low-temperature GPC light scattering responses for filtered samples of a-PP and the THF-extracted component of its TAM derivatives C–G (Table 1).

Optical microscopy studies of the product under steady-shear conditions using phase-contrast filters (not shown) revealed a free-flowing, grainy morphology, but individual particles could not be resolved at this magnification. Therefore, the product was extracted repeatedly with toluene, sonicated as an acetone suspension, and dispersed on a glass slide. Residual material amounted to less than 1 wt% of the reaction mixture, which SEM imaging showed to be particles with dimensions on the order of 50–100 nm, as well as micron-sized aggregates derived from these primary particles (Fig. 5). They were sufficiently cross-linked that they were not prone to coalescence. Pressing the particles at 200 °C gave an opaque, white film that dispersed completely when sonicated in acetone.

Elemental analysis differentiated these particles from all the reaction products described to this point. The polymerization of pure TAM using DCP as initiator gave a translucent, glassy solid with an elemental composition of C: 65.7%, H: 5.6%, O: 27.8%. This correlates to the expected TAM content of 96%. Analysis of the particles derived from an a-PP reaction showed relatively little hydrocarbon enrichment, with a mass composition of C: 69.7%, H: 7.9%, O: 20.9% that equates to a TAM content of 72 wt%. The remaining 28 wt% could amount to no more than an average of three propylene mers per molecule of TAM. Given that the molecular weight of PP chains was on the order of 4 K, it is clear that these particles do not contain a high mole fraction of PP. It is likely that methyl and cumyloxyl initiator fragments are incorporated as well as small amounts of PP. The nature of this precipitation polymerization process will be explored in Section 4.

3.2. High molecular weight isotactic-PP derivatives

We found that high molecular weight starting materials tend to generate expansive gel fractions. The outcome of reacting a high viscosity i-PP homopolymer ($M_n = 70{,}700$ g/mol) with 0.4 wt% DCP and 6.0 wt% is summarized in Scheme 2. The crude product showed evidence of graininess when examined in the melt state using an optical microscope, and three components were isolated by solvent extraction. The majority fraction dissolved readily in refluxing xylene, with just 6 wt% of material retained by a wire mesh extraction. This retained hyper-branched gel contained a large amount of converted TAM (Scheme 2), and coalesced into a featureless, translucent polymer film when pressed at 200 °C. It was exceedingly difficult to isolate particles from this gel, and we cannot

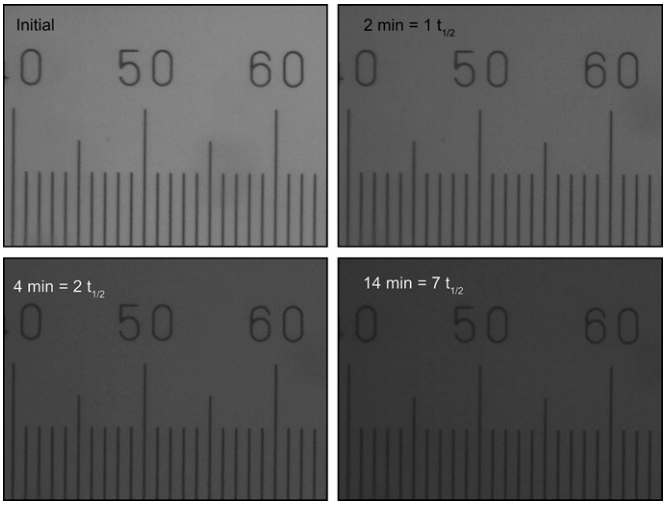

Fig. 4. Optical transmission images of an a-PP-*g*-TAM reaction at $t = 0$ min, 2 min, 4 min, and 14 min. (Experiment E, Table 1, scale division = 0.1 mm, 40× magnification.)

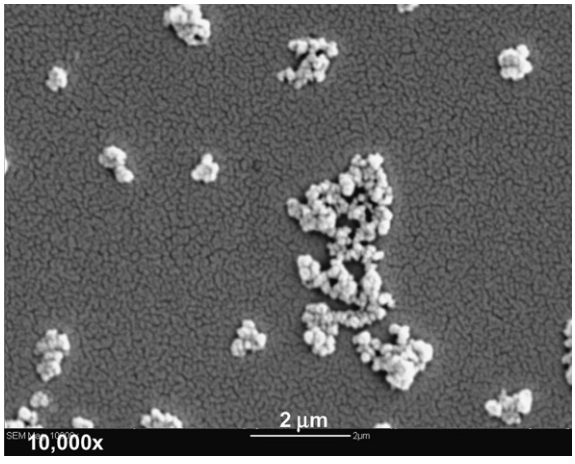

Fig. 5. SEM image of particles isolated from Experiment G, Table 1.

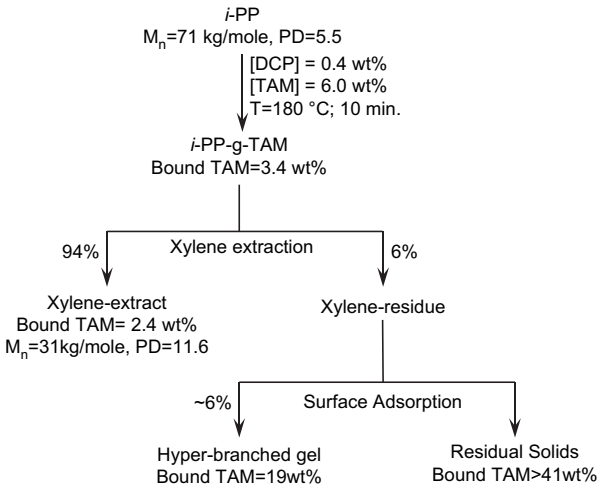

Scheme 2.

provide an accurate estimate of particle yield. SEM analysis of residual solids revealed spheres with aggregate sizes on the order of 1 μm, and elemental analysis reported a TAM content of 41 wt%. We believe this to be a minimum value, given the likelihood of contamination by hyper-branched gel.

The xylene-soluble component of i-PP-*g*-TAM was subjected to high-temperature GPC analysis to produce the refractive index, intrinsic viscosity and light scattering profiles which are plotted in Fig. 6. The data reveal the extent to which the soluble matrix of i-PP-*g*-TAM was degraded by the modification process, as its M_n was reduced by more than half (Scheme 2). Such severe matrix degradation was not observed in the a-PP-*g*-TAM system, where a low substrate molecular weight and the limited kinetic chain length of scission and allylic ester addition left the matrix relatively untouched. In this high molecular weight i-PP example, reaction yields were sufficient to affect the great majority of polymer chains, with fragmentation exceeding the extent of TAM-induced cross-linking.

That a TAM-based modification of high molecular weight PP yielded a small gel fraction and a *degraded* polymer matrix is clear evidence of a bimodal molecular weight distribution. High-temperature GPC analysis of the xylene-soluble fraction of i-PP-*g*-TAM supported this observation, while providing further insight into the product's branching distribution (Fig. 6). With virtually all of the TAM-rich gels removed, there remained a small amount of high molecular weight, hyper-branched material within the i-PP-*g*-TAM extract. The intrinsic viscosity of this polymer fraction is of particular interest, since it showed a remarkable negative deviation from the parent material. This is consistent with a branched architecture that is localized within the high molar mass chain population [17]. We can conclude, therefore, that i-PP-*g*-TAM possesses bimodal molecular weight and branching distributions, with a majority population of essentially linear, degraded chains and a minority population of hyper-branched chains whose mass can extend beyond the gel point.

4. Discussion

4.1. Evolution of molecular weight and branching distributions

Radical activity on a polypropylene chain is generated by hydrogen atom donation by the polymer to initiator fragments, monomer-derived radical intermediates, and other polymeric macroradicals. Since the probability of hydrogen atom transfer is essentially uniform between propylene mers, chains of higher molecular weight are engaged preferentially. This is the basis of well-established "controlled-rheology" polypropylene technology, which uses macroradical fragmentation to cleave the largest chains within the MWD disproportionately, thereby reducing polydispersity [16,18].

Radical-mediated cross-linking of ethylene-rich polyolefins in the absence of coagents has also been the subject of considerable experimental and theoretical analyses. It is known that radical activity is more intense amongst the largest chains, and that radical–radical termination by combination builds molecular weight disproportionately within the high-mass population [19]. The resulting distribution of cross-links is skewed to the extent that a gel condition is reached before a substantial fraction of the polyolefin is modified whatsoever. In a coagent-mediated system, this molecular weight amplification is more intense, since cross-linking distributions are not the sole products of random hydrogen atom abstraction events. Coagent is preferentially grafted to high

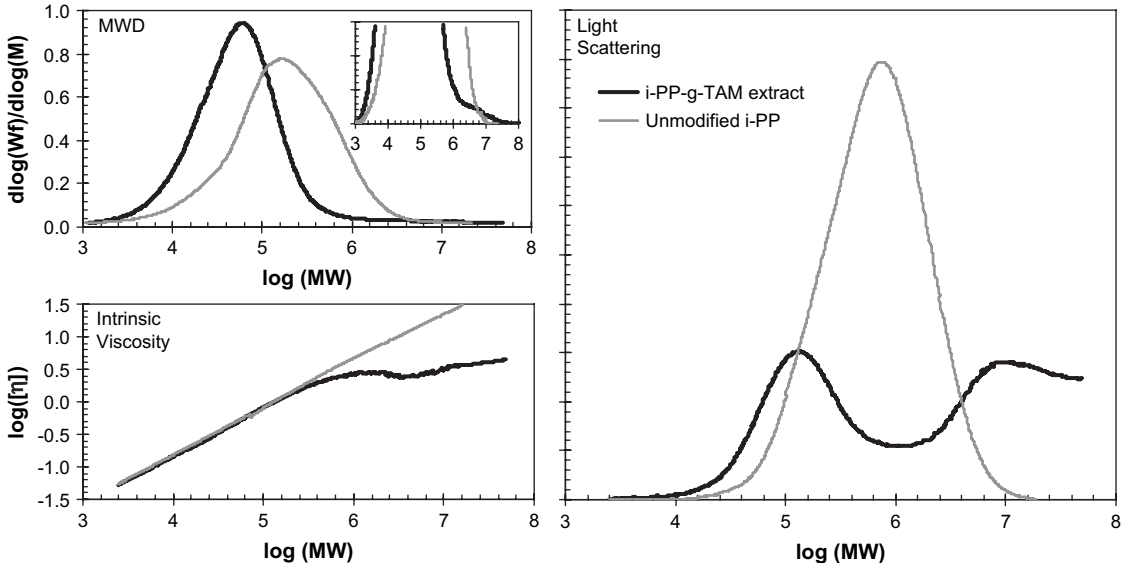

Fig. 6. High-temperature GPC molecular weight distribution, Mark–Houwink plot, and light scattering detector response profiles for unmodified i-PP and the xylene-soluble fraction of its i-PP-*g*-TAM derivative (Scheme 2).

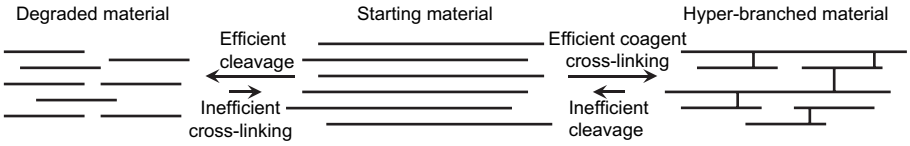

Scheme 3. Simplified representation of coagent-induced bimodality.

molecular weight chains, which in turn will have a heightened capacity for cross-linking through further additions to bound C=C functionality.

Based on these arguments, bimodal branching and molecular weight distributions are expected to evolve with the degree of simultaneous chain scission and TAM activation (Scheme 3). Recognize that an average linear chain is readily cleaved, but the low molecular weight of the resulting fragments makes them less likely to engage in TAM-assisted cross-linking. Conversely, average linear chains that are branched through TAM addition are difficult to cleave effectively. As the branching extent increases within this population, the distribution of polymer scission products becomes skewed toward small chains and large, branched fragments [20]. The impact of chain cleavage on molecular weight declines, and the tendency for cross-linking to overwhelm fragmentation is amplified to the point where no practical amount of radical-mediated polymer degradation can alter the molecular weight of a hyper-branched fraction.

In our low molecular weight a-PP system, the entire chain population could not be affected by the modification process, given the low kinetic chain length of scission and cross-linking reactions, and the small amount of initiator used relative to the number of a-PP chains in the reaction mixture. GPC and NMR analyses showed that the matrix was mostly untouched, while the hyper-branched chain population became more abundant as TAM conversion increased. The high initial molecular weight of our i-PP system resulted in a different product distribution. With an order of magnitude fewer chains per gram, radical activity accessed the whole chain population to yield a branched matrix with a M_n lower than the starting material, and an expansive gel fraction.

We cannot rule out the possibility that functional group aggregation contributes to the bimodal structure of PP-*g*-TAM products [21]. The association of coagent-modified chains would concentrate large, branched structures, whose intermolecular reactions would support the explosive molecular weight growth that is needed to build a 200 kg/mol hyper-branched a-PP structure from a 5 kg/mol starting material. In the absence of such branched chain interactions, molecular weight increases would proceed in 5 K or 10 K increments – a much less efficient growth mechanism.

4.2. Particle formation

Our discovery of non-sinterable particle generation during the graft modification of PP is, to the best of our knowledge, without precedent. However, parallels exist between the TAM-mediated process observed in this work and well-documented observations of precipitation polymerization. The studies of Stöver and coworkers [22] on the production of micro-spheres from homogeneous styrenic monomer solutions containing divinylbenzene are relevant, since they demonstrate the stability conferred on particles by cross-linking, and they highlight the sensitivity of particle formation to solvent polarity, reagent concentrations, and reaction conversions.

We showed previously that the predominant mode of allylic ester activation in dilute cyclooctane and a-PP solutions is a chain process that is dominated by C–H bond addition to olefin [8]. This simple grafting pathway generates the hyper-branched PP structures revealed in this study. With C=C functionality scarce compared to C–H bonds, hydrogen atom donation by the polymer to radical intermediates is more favourable than repeated allyl group addition (Scheme 1). However, the importance of oligomerization rises dramatically under TAM-rich conditions, as evidenced by our polymerization of neat TAM into an insoluble, glassy solid.

Since mixtures of 3.0 wt% coagent in a-PP are homogeneous solutions at 170 °C, a dispersed TAM-rich phase can only result from reaction-induced phase instability [23]. That is, coagent activation must generate insoluble adducts that separate into a dispersed phase, and cross-link to form non-sinterable particles. Given that our nano-particles contain very little hydrocarbon, this process may arise from a direct attack of peroxide-derived radicals on TAM. The structure and phase behaviour of these insoluble intermediates are the subjects of a continuing study.

5. Conclusions

The peroxide-mediated grafting of TAM to PP is dominated by a conventional propagation sequence of radical addition/hydrogen atom transfer. The distribution of cross-links and fragmentation products amongst PP chains evolve toward bimodality as the balance of coagent-assisted cross-linking and radical-mediated fragmentation shifts with polymer architecture. In high molecular weight PP-*g*-TAM systems, products are comprised of a dominant lightly branched fraction of reduced molecular weight, and a minor, hyper-branched fraction whose molecular weight can exceed the gel point. Reaction-induced phase separation of TAM adducts operates concurrently with PP modification to produce a small yield of cross-linked nano-particles.

Acknowledgements

Financial support from the Natural Sciences and Engineering Research Council (NSERC) and The Dow Chemical Company is gratefully acknowledged.

References

[1] (a) Hingmann R, Marczinke BL. J Rheol 1994;38:573–87;
(b) Auhl D, Stange J, Munstedt H, Krause B, Voigt D, Lederer A, et al. Macromolecules 2004;37:9465–72;
(c) Spitael P, Macosko CW. Polym Eng Sci 2004;44:2090–100.
[2] Stange J, Uhl C, Munstedt H. J Rheol 2005;49:1059–79.
[3] Weng W, Hu W, Dekmezian AH, Ruff CJ. Macromolecules 2002;35:3838–43.
[4] (a) Nam GJ, Yoo JH, Lee JW. J Appl Polym Sci 2005;96:1793–800;
(b) Yoshii F, Makuuchi K, Kikukawa S, Tanaka T, Saitoh J, Koyama K. J Appl Polym Sci 1996;60:617–23.
[5] (a) Graebling D. Macromolecules 2002;35:4602–10;
(b) Kim BK, Kim KJ. Adv Polym Tech 1993;12:263–9.
[6] (a) Borsig E, Fiedlerova A, Lazar M. J Macromol Sci Chem 1981;A16:513–28;
(b) Han DH, Shin SH, Petrov S. Radiat Phys Chem 2004;69:239–44.
[7] Zhang L, Guo B, Zhang Z. Gaodeng Xuexiao Huaxue Xuebao 2001;22(8):1406–9.
[8] Sengupta SS, Parent JS, McLean JK. J Polym Sci Part A Polym Chem 2005;43:4882–3.
[9] Litt M, Eirich FR. J Polym Sci 1960;45:379–96.
[10] Muenger K, Fischer H. Int J Chem Kinet 1985;17:809–29.
[11] Zytowski T, Fischer H. J Am Chem Soc 1996;118:437–9.
[12] Bartlett PD, Altschul R. J Am Chem Soc 1945;67:816–22.

[13] Bartlett PD, Tate FA. J Am Chem Soc 1953;75:91–5.
[14] Coiai S, Passaglia E, Aglietto M, Ciardelli F. Macromolecules 2004;37:8414–23.
[15] Cartier H, Hu G. J Polym Sci Part A Polym Chem 1998;36:1053–63.
[16] Tzoganakis C, Vlachopoulos J, Hamielec AE. Polym Eng Sci 1989;29:390–6.
[17] Gabriel C, Munstedt J. Rheol Acta 2002;41:232–44.
[18] Ryu SH, Gogos CG, Xanthos M. Adv Polym Tech 1992;11:121–31.
[19] (a) Saito O. In: Dole M, editor. Radiation chemistry of macromolecules, vol. 1. New York: Academic Press; 1972. p. 223–61;
(b) Tobita H. J Polym Sci Part B Polym Phys 1995;33:1191–202;
(c) Tobita H. Macromol Theory Simul 1998;7:225–32.
[20] (a) Guidici R, Hamielec AE. Polym React Eng 1996;4:73–101;
(b) Kim DM, Busch M, Hoefsloot HCJ, Iedema PD. Chem Eng Sci 2004;59:699–718.
[21] (a) de Lucca Freitas LL, Stadler R. Macromolecules 1987;20:2478–85;
(b) Lee JA, Kontopoulou M, Parent JS. Polymer 2004;45:6595–600.
[22] (a) Downey JS, Frank RS, Li WH, Stover HDH. Macromolecules 1999;32:2838–44;
(b) Downey JS, McIsaac G, Frank RS, Stover HDH. Macromolecules 2001;34:4534–41.
[23] (a) Fredrickson GH, Liu AJ, Bates FS. Macromolecules 1994;27:2503–11;
(b) Fredrickson H, Liu AJ. J Polym Sci Part B Polym Phys 1995;33:1203–12.